Published in final edited form as:
Integr Biol (Camb). 2010 September ; 2(9): 424–434. doi:10.1039/c0ib00040j.

Endogenous patterns of mechanical stress are required for branching morphogenesis

Nikolce Gjorevski[a] and **Celeste M. Nelson**[a,b,1]

[a]Department of Chemical & Biological Engineering, Princeton University, Princeton, NJ 08544

[b]Department of Molecular Biology, Princeton University, Princeton, NJ 08544

Abstract

Spatial patterning of cell behaviors establishes the regional differences within tissues that collectively develop branched organs into their characteristic treelike shapes. Here we show that the pattern of branching morphogenesis of three-dimensional (3D) engineered epithelial tissues is controlled in part by gradients of endogenous mechanical stress. We used microfabrication to build model mammary epithelial tissues of defined geometry that branched in a stereotyped pattern when induced with growth factors. Branches initiated from sites of high mechanical stress within the tissues, as predicted numerically and measured directly using 3D traction force microscopy. Branch sites were defined by activation of focal adhesion kinase (FAK), inhibition of which disrupted morphogenesis. Stress, FAK activation, and branching were all altered by manipulating cellular contractility, matrix stiffness, intercellular cohesion and tissue geometry. These data suggest that the pattern and magnitude of mechanical stress across epithelial tissues cooperate with biochemical signals to specify branching pattern.

Insight, innovation, integration—Morphogenesis is ultimately a physical process wherein tissues are sculpted into their final three-dimensional (3D) patterns. Mechanical stresses from the microenvironment can also play regulatory roles, but their influence on pattern is difficult to ascertain in 3D systems in vivo. Here we *integrate* 3D microscale engineered tissues with *insight* from biological mechanics to understand the role of endogenous mechanical stresses in patterning tissue development. The *innovation* lies in the use of numerical modeling to design experiments that can predict the stress distribution and resulting morphogenesis of model tissues.

Keywords

ECM; biomechanics; force; FAK; micropatterning; mechanotransduction

Introduction

Branching morphogenesis is a striking example of complex tissue architecture arising from spatially patterned cell behavior. Subgroups of cells are instructed to form nascent branches and invade the surrounding stroma while neighboring cells remain quiescent. A number of biochemical signals – growth factors, proteases, extracellular matrix (ECM) molecules and morphogens[1, 2] – act as global regulators of branching morphogenesis in vivo and in culture. Nevertheless, the local regulators that determine branch initiation points and the spacing between ducts remain obscure[3]. Advances in engineering three-dimensional (3D) tissues have opened the possibility of using organotypic tissue mimetics to study such complex

[1]Address correspondence to C.M.N., A321 Engineering Quadrangle, Princeton, NJ 08544, Tel: 609 258 8851, celesten@princeton.edu.

developmental programs quantitatively[4]. To delineate the local regulators of branching, we recently developed an engineered tissue model of the mammary epithelial duct comprised of mouse mammary epithelial tubules of precisely defined geometry surrounded by collagen gel[5, 6]. Although it does not completely replicate the histology of the mammary gland, this technique generates thousands of engineered tissues of identical size, shape, and branching pattern, making it useful for identifying the signals that influence branch initiation sites. Branching of the engineered tubules was inhibited by high concentrations of autocrine-secreted transforming growth factor (TGF)-β[5], confirming a long-standing hypothesis in the field[7]. Branch sites in vivo and in culture thus appear to be controlled in part by concentration gradients that form in the surrounding microenvironment.

In addition to biochemical cues, tissues are exposed to cues of biophysical nature, including substratum stiffness and cytoskeletal tension, which control key morphogenetic processes such as proliferation, apoptosis, and differentiation[8–12]. Recent studies have also suggested a role for the mechanical environment in the development of branched tissues[13–16]. Down-regulating contractility in the embryonic lung results in decreased branching[14] whereas up-regulating contractility promotes branching[13]. Similarly, disrupting stress fiber formation and tissue contractility inhibits branching in the kidney and results in a dysmorphic organ[17]. In the lung, salivary gland, and mammary gland, the basement membrane thins out adjacent to emerging branches[14, 18, 19], consistent with the hypothesis that mechanical stresses are concentrated at future sites of branching and influence matrix turnover and morphogenesis[20]. Mechanical stresses arise from the isometric contraction of individual cells, but become concentrated into patterns as a result of asymmetries in the geometry of the tissue, as demonstrated in amphibian embryos[21] and in two-dimensional (2D) cultured epithelial sheets[11]. We thus set out to test whether the pattern of branching is templated by endogenous patterns of mechanical stress.

Here we used numerical and engineered culture models to investigate the role of endogenous mechanical stress in the patterning of branching morphogenesis. We show experimentally that mechanical stress is distributed non-uniformly across 3D model epithelial tissues. Branching occurs at regions of high stress, and changes in the extent of branching correlate with changes in the magnitude of stress at branching sites. Endogenous stress activated focal adhesion kinase (FAK), inhibition of which prevented branching of the model tissues. These results suggest that mechanical stresses and biochemical signals from the microenvironment cooperate to determine sites of branching.

Results

Mechanical stress is distributed non-uniformly across model epithelial tissues

To investigate whether patterns of mechanical stress were present within morphogenetic epithelia, we used the finite element method (FEM) to solve a computational model of an epithelial tubule contracting within a compliant ECM gel (Fig. 1A). We simulated contraction by the epithelium and computed the resulting maximum principal stress within the tissue. The elastic moduli of the epithelial and ECM portions of the model were chosen to match those of normal mammary cells and tissue[15, 22].

For cylindrical tubules, the FEM model predicted that stress would be distributed non-uniformly and concentrated at the tips of the tubules (Fig. 1B,C). To verify the predicted stress experimentally, we took advantage of the fact that regions experiencing higher mechanical stress store more elastic strain energy. Relaxing the strain results in displacement of the matrix; the magnitude of displacement correlates with the local magnitude of stress[23, 24]. We used a microfabrication approach to engineer mammary epithelial tubules of size and geometry corresponding to those of the FEM model, embedded

in a collagenous matrix[5, 6]. Matrix displacement was monitored by incorporating fluorescent beads within the surrounding collagen gel (Fig. 1D). Cell relaxation resulted in non-uniform displacement of the beads around the tubules (Fig. 1E,F). Larger displacements were recorded at the tips than at the trunks, indicating that stress was concentrated at the tips of the tubules, consistent with the predictions of the FEM model. Adding hepatocyte growth factor to the engineered tubules induced multicellular branches to invade into the surrounding collagen in a highly patterned fashion from the tips of the tubules (Fig. 1G–L), as reported previously[5]. Comparing the stress distribution and branching profiles reveals that branches emerge from regions that experience elevated stress.

Cellular contractility regulates mechanical stress and branching morphogenesis

To define the role of mechanical stress in branching morphogenesis, we perturbed the stress experienced by the tissue by modulating cellular contractility both numerically and experimentally. Varying the contractility of the epithelium in the FEM model had no effect on the relative patterns of simulated stress, but increasing contractility led to a higher magnitude of stress at the tips of the tubules (Fig. 2A–D). Based on these results, we examined how modulating cellular contractility affected mechanical stress and branching morphogenesis of the engineered tubules. Contractility of the actomyosin cytoskeleton is regulated in part by signaling through RhoA, its effector Rho kinase (ROCK), and myosin light chain kinase (MLCK). Reducing contractility with the ROCK inhibitor Y27632[25] or increasing contractility with the myosin light chain phosphatase inhibitor calyculin A[26] had no effect on the pattern of stress or branching (Fig. 2E–K). However, as contractility increased the magnitude of stress and extent of branching (the fraction of tubules that branched) from the tips increased (Fig. 2H,L). Branching also correlated with contractility when tubules were transduced with dominant negative (RhoA-N19) or constitutively active (RhoA-L63) RhoA (Fig. 2M–P). Similar results were obtained using the MLCK inhibitors ML-7 and BDM and the phospholipid mediator lysophosphatidic acid (LPA) (Supp. Fig. 1). Although proliferation and cell motility are required for branching in this system[5], neither was inhibited by manipulating contractility (Supp. Figs. 2–3). These results are consistent with the FEM predictions: as cellular contractility increases, the patterns of stress and branching remain unchanged, but the magnitudes of stress and branching both increase.

Matrix stiffness regulates mechanical stress and branching morphogenesis

The mechanical properties of a tissue are defined by the contractility of the cells as well as by the compliance of the surrounding ECM. Stiff ECM disrupts the tubulogenesis of mammary epithelial cells[16] and induces proliferation, invasion and loss of mammary epithelial architecture[15, 27, 28]. Matrix elasticity has also been shown to control membrane protrusions by individual endothelial cells[29] and growth factor receptor expression and sprouting during blood vessel morphogenesis[30]. To examine the effect of ECM compliance on the stress profile within the tissue, we performed simulations in which we varied the elastic modulus of the matrix portion of the FEM model. Increasing matrix stiffness increased the magnitude of stress but had no effect on the pattern (Fig. 3A–C). We examined the effect of ECM compliance on branching morphogenesis experimentally by varying the stiffness of the collagen surrounding the engineered tubules by crosslinking with D-ribose[31] (Fig. 3G). The elastic moduli of the crosslinked gels corresponded to the moduli of the matrix within the FEM model. Increasing the stiffness of the matrix had no effect on the pattern of branching but enhanced branching from the tips (Fig. 3D–F). Thus, as the matrix becomes stiffer the patterns of mechanical stress and branching remain unchanged, but the magnitudes of stress and branching both increase.

Intercellular cohesion governs mechanical stress and branching of epithelial tissues

Individual cells within tissues are mechanically coupled to their neighbors via cadherin-mediated intercellular adhesions[32], and perturbing these connections has been found to prevent the transmission and concentration of mechanical stress[11]. To disrupt the transmission of stress between cells within the tubules, we expressed a dominant-negative mutant of E-cadherin (EΔ) that blocks connection to the actin cytoskeleton by inhibiting the junctional localization of β-catenin[33] (Fig. 4A,B). Expression of EΔ resulted in a flattened stress profile across the tubules, as determined by evaluating the displacements of beads in the collagen surrounding the tubules (Fig. 4C,D). Expression of EΔ completely prevented branching (Fig. 4E,F) without inhibiting cell proliferation or motility (Supp. Fig. 4–5). These data suggest that branching requires transmission of mechanical stress.

Focal adhesion kinase activity is non-uniform across epithelial tissues

Focal adhesion kinase (FAK) integrates a number of extracellular cues to control ECM adhesion and cell migration[34]. Deletion of FAK retards mammary ductal elongation[35] and causes aberrant branching morphogenesis[36]. These findings, along with evidence that mechanical stress activates FAK by phosphorylation at Y397[37, 38], led us to examine the role of FAK in the mechanical regulation of branching morphogenesis. Immunofluorescence analysis revealed that FAK phosphorylation was increased at the tips of the tubules (Fig. 5A,B), consistent with our experimental and computational findings that cells in these regions also experienced the highest stress. To test directly whether FAK regulates branching of the engineered tubules, we expressed FAK Dter, a dominant-negative mutant that lacks the kinase domain[39]. Cells that expressed FAK Dter showed reduced phosphorylation of Y397 at cell-matrix adhesions (Fig. 5C,D) and a homogeneously low level of FAK phosphorylation across the tubules (Fig. 5E,F). Furthermore, FAK Dter-expressing tubules failed to undergo branching morphogenesis (Fig. 5G,H). However, expression of FAK Dter had no effect on cell proliferation or motility within the tubules (Supp. Fig. 4–5). As expected, treatment with pharmacological agents that inhibited actomyosin contractility and branching decreased phosphorylation of FAK Y397, whereas phosphorylation was increased upon treatment with agents that activated contractility and branching (Fig. 5I; Supp. Fig. 6). Furthermore, stiffening the collagen matrix, which increased extent of branching (Fig. 3), enhanced the phosphorylation of FAK Y397 at the ends of the tubules (Fig. 5J,K). These data suggest that mechanical stress regulates branching in part by activating FAK.

Tissue geometry patterns mechanical stress and branching morphogenesis

Recent studies have established a relationship between the geometry of 2D epithelial sheets and their patterns of endogenous mechanical stress[11, 40]. To determine how geometry affects mechanical stress and branching morphogenesis of 3D epithelial tissues we varied the initial tubule shape. Changing the shape altered the predicted distribution of mechanical stress across the tissue, with regions of high convex curvature experiencing the highest stress (Fig. 6A–C, M–O). Immunofluorescence analysis of engineered tubules of the corresponding geometries showed that activated FAK was concentrated in the high stress regions (Fig. 6D–F). Branching assays revealed a partial match between the patterns of stress and branching (Fig. 6G–I): regions of low stress were prevented from branching, but not all high stress regions branched (asterisks in Fig. 6H,I). This apparent discrepancy can be explained by considering the concentration profile of TGFβ, an epithelial-secreted morphogen that inhibits branching morphogenesis in this system[5]. An FEM model of TGFβ secretion and diffusion predicted that every high stress region that failed to branch was exposed to high concentrations of TGFβ (Fig. 6J–O). These results suggest that high mechanical stress is necessary but not sufficient for branching: when cells within the engineered tissues are

presented with opposing mechanical and biochemical cues, the biochemical signal (i.e. TGFβ) dominates the resulting phenotype.

Discussion

Spatial non-uniformities of mechanical stress have previously been reported in 2D epithelial sheets[11, 40]. Here, we predicted computationally and demonstrated experimentally that 3D model epithelial tissues experience patterns of endogenous mechanical stress that are dictated by the initial shape of the tissue. Although cytomechanical factors have been implicated in the morphogenesis of the lung[14] and kidney[17], the regulation of branching pattern has been traditionally ascribed to biochemical and genetic factors[1, 41]. Indeed, we recently demonstrated that the concentration profile of the autocrine inhibitory morphogen TGFβ acts locally to control morphogenesis by preventing spurious branching[5]. Here, we showed that mechanical stress is elevated at branch sites, which suggests that mechanical gradients may also play a role in the patterning of branching morphogenesis. It is important to note, however, that branching only occurred at locations where the biochemical and mechanical cues were predicted to reinforce each other. Sites were prevented from branching when provided with the stimulatory cue of high mechanical stress and the inhibitory cue of high TGFβ concentration. Conversely, low TGFβ concentration failed to permit branching when mechanical stress was removed pharmacologically. We found also that the magnitude of mechanical stress at branching sites correlated with the extent of branching: decreasing the magnitude of stress by decreasing cellular contractility or matrix stiffness resulted in decreased branching, whereas increasing the magnitude of stress resulted in increased branching.

How might mechanical stress regulate branching morphogenesis? Possible mechanisms include removal of steric hindrances by matrix degradation and enhanced cellular motility and invasiveness. Branch initiation in the lung[14], salivary gland[18], and mammary gland[19] is preceded by local thinning of the basement membrane, which is thought to remove a physical obstacle, thus allowing the adjacent epithelium to invade in a fashion analogous to a “run in a stocking”[42]. Matrix turnover at branching sites has been attributed to a stress-induced local increase in the production of ECM-degrading matrix metalloproteinases (MMPs)[14]. This local increase in MMP activity, however, necessitates the pre-existence of spatial non-uniformities in mechanical stress. In the present study we demonstrated that such mechanical gradients can arise within a model epithelial tissue from intercellular transmission of stress along the tissue geometry. Furthermore, MMP14 is elevated at the leading edge of mouse mammary and ureteric ducts [43–45] and at the tips of engineered mammary tubules[46]. Inactivation of the Rho pathway abolishes both elevated MMP14[46] and branching from the tips. Stress-induced branching may thus proceed through local stimulation of MMP activity[47, 48].

High local stress could also activate a mechanically-sensitive signaling pathway resulting in enhanced cellular motility and invasion. Our observation of elevated levels of active FAK at branch sites, along with the finding that FAK activity is necessary for branching, suggests that high mechanical stress might induce branching morphogenesis in part through activation of FAK. At the cellular level, FAK regulates migration and invasion by causing membrane protrusions and focal adhesion turnover (reviewed in [34, 49]). At the tissue level, deletion of FAK disrupts normal development of the mammary gland[35, 36] and lung bronchioles[50]. Conversely, tissue stiffness was found recently to activate FAK and induce invasion of mammary epithelial cells in culture and *in vivo*[27]. Activated FAK could thus regulate branching by promoting migratory and invasive behavior at the tips of the tubules.

High mechanical stress may also result in gene expression changes at nascent branch sites. Expression of mesenchymal markers such as Twist-1, Twist-2 and Snail has been observed in the tip regions of mouse mammary ducts[51] and at future branching sites in engineered mammary tubules[5]. The roles of these genes in branching morphogenesis, as well as the factors that influence their localized expression patterns, remain to be determined. However, we recently found that mechanical stress induces patterned epithelial-mesenchymal transition (EMT) in 2D epithelial monolayers[40]; a similar phenomenon may occur in the context of 3D epithelial tissues undergoing morphogenesis into collagenous ECM. It is important to emphasize that TGFβ is probably not responsible for the expression of mesenchymal markers in the branching tubules. Although TGFβ is a potent promoter of EMT in mammary epithelium containing an oncogenic or disruptive stimulus[52, 53], the overwhelming majority of normal mammary epithelial cells, including those used here, do not undergo EMT upon treatment with TGFβ[54, 55]. Indeed, we have previously demonstrated that the spatial profile of TGFβ correlates inversely with the locations at which mesenchymal markers are expressed within our model tissues[5]. Further studies are required to define the gene expression changes at branch initiation sites, which may be the junction at which mechanical and biochemical signals are integrated during branching morphogenesis.

It is well accepted that mechanical changes accompany and drive malignant transformation and progression within branched organs such as the breast and lung[56, 57]. To our knowledge, the work presented here provides the first experimental confirmation that mechanical stress is altered at branch initiation sites in multicellular aggregates, and supports the hypothesis that mechanical stress also dynamically orchestrates the normal morphogenesis of treelike tissues[3, 42]. Finally, the results of this study, implicating mechanical stress as a regulator of organogenesis, underscore the need to consider endogenous multicellular mechanics in tissue engineering strategies aimed at faithfully reconstructing these organs *ex vivo*.

Materials and Methods

Cell culture and reagents

Functionally normal EpH4 mouse mammary epithelial cells were cultured in 1:1 Dulbecco's Modified Eagle's Medium: Ham's F12 nutrient mixture (DMEM:F12) (Hyclone), 2% fetal bovine serum (Atlanta Biologicals), 5 μg/ml insulin (Sigma), 50 μg/ml gentamycin (Sigma). Tubules were treated upon induction of branching with Y27632 (Tocris), calyculin A (Calbiochem), cytochalasin D (Tocris), ML7 (Calbiochem), BDM (Calbiochem), or LPA (Cayman Chemical) diluted to the concentrations indicated in the text. Recombinant adenoviruses encoding E-cadherin lacking the β-catenin-binding domain (EΔ) and mutant FAK lacking the autophosphorylation site (FAK Dter) were gifts from Christopher Chen (University of Pennsylvania) and Lewis Romer (Johns Hopkins University), respectively. Recombinant adenoviruses encoding RhoA-N19 and RhoA-L63 were obtained from Cell Biolabs. High titer preparations of recombinant adenoviruses were generated using the AdEasy Virus Purification Kit (Stratagene). Cells were transduced at an MOI resulting in >99% transduction efficiency.

Microfabrication

Elastomeric stamps of poly(dimethylsiloxane) (PDMS; Sylgard 184, Ellsworth Adhesives) containing the desired geometries in bas-relief were fabricated by a combination of photolithography and soft lithography[5, 6]. Stamps were rendered non-adhesive by coating with 1% bovine serum albumin (BSA) in phosphate-buffered saline (PBS). Modified stamps were placed atop a drop of neutralized liquid collagen (Koken, Japan) which was then gelled at 37°C. Stamps were removed and a suspension of mammary epithelial cells was allowed to settle within the molded collagen cavities. The extra cells were washed away with culture

medium and a gelled collagen “lid” was placed on top of the pattern. The epithelial cells adopted the shape and size of the collagen cavities they occupied, forming tubules that remained quiescent until they were induced to branch by adding hepatocyte growth factor (5 ng/ml; Sigma). Within 24 h after growth factor addition, multicellular branches invaded the surrounding collagen matrix. To increase the stiffness of the collagen surrounding the tubules, the molded gels were crosslinked by incubation in D-ribose at 37°C for one week prior to adding cells.

Measurement of matrix displacements

To visualize displacements within the collagen matrix, 1-μm diameter fluorescent microbeads (Invitrogen) were mixed with the neutralized liquid collagen. The positions of the beads in a single plane were recorded before and after relaxing the tubules with 0.05 % Triton X-100 in PBS. The displacement maps were generated using the Imaris tracking software (Bitplane). To validate that greater displacements corresponded to greater stress, we used the displacement maps to calculate the average strain (which is proportional to the average stress) at the midsection and ends of the tubules.

Rheometry

The rheological measurements of collagen gels hydrated with culture media were performed on a Physica MCR 501 rheometer (Anton Paar) with cone-and-plate geometry. The chamber was held at 37°C and 100% humidity using a Peltier plate and humidity chamber. All measurements were performed in the linear viscoelastic regime (0.01–3% strain, 0.1–25 rad/sec angular frequency). The measured storage modulus (G') was used to compute Young’s modulus (E) using $E = 2G'(1+\nu)$, assuming a Poisson ratio ν of 0.2[58].

Imaging and immunofluorescence analysis

To quantify the magnitude and pattern of branching, samples were fixed, stained for nuclei with Hoechst 33258 (Invitrogen), and visualized using a Hamamatsu Orca 1394 camera attached to a Nikon Eclipse Ti microscope at 10× magnification. The binarized images of ~50 tubules were stacked with Scion Image software to obtain a pixel frequency map, which was subsequently color-coded in Adobe Photoshop. All experiments were conducted at least three times. The extent of branching was also quantified by measuring the pixel intensity within frequency maps at a location 12 μm from the tips of the initial tubule for the three replicates of each condition. The averaged pixel intensities at these locations were divided by the pixel intensity at the trunk of the tubule (corresponding to cell frequency of 100%) to yield the percent of tubules that have extended branches. Values less than 5% were considered to be noise arising from misalignment during stacking.

For immunofluorescence analysis of β-catenin and E-cadherin, samples were washed in PBS and fixed in 4% paraformaldehyde for 15 min at room temperature. Samples were permeabilized with 0.1% Triton X-100 in PBS (PBS-T) for 15 min and blocked for 1 h at room temperature in 10% goat serum in PBS (PBS-S), followed by overnight incubation in primary antibody recognizing β-catenin (Sigma) or E-cadherin (Cell Signaling) at 1:100 dilution in PBS-S. Samples were washed extensively with PBS and incubated in secondary antibody cocktail at 1:1000 in PBS-S for 1 h at room temperature.

For immunofluorescence analysis of FAK pY397, samples were washed in PBS and fixed in 4% paraformaldehyde for 15 min at room temperature. Samples were permeabilized 2 × 10 min in 0.5% Igepal Ca-630 and incubated in PBS-T for 15 min. Samples were blocked overnight at 4°C in PBS-S, followed by overnight incubation at 4°C in primary antibody recognizing FAK pY397 (Invitrogen) at 1:100 dilution in PBS-S. Samples were washed

extensively with PBS and incubated in secondary antibody at 1:1000 in PBS-S overnight at 4°C. Frequency maps were constructed from fluorescence images as described above.

Proliferating cells were visualized with the Click-iT EdU Imaging Kit (Invitrogen) as previously described[46]. Frequency maps of cell proliferation were constructed from fluorescence images as described above.

Numerical modeling

A 3D computational model of the engineered tubules was solved for the profile of mechanical stress using the finite element method (FEM) in Comsol Multiphysics 3.5a software (Comsol Inc). For conciseness, we report the maximum principal stress across the tissues. No shear stresses exist in the principal directions at any point of the tissues. Thus, the highest of the three principal stresses (all normal) summarizes the stress state at that point in a single quantity. The epithelial tubules of varying geometry were represented as a contractile shell 10 μm thick[59] with Young's modulus of 500 Pa[22] and Poisson ratio of 0.499 (practically incompressible). An equilibrium state was assumed and a zero pressure drop across the shell was prescribed. The tubule was embedded in a passive compliant slab of cylindrical geometry (2 mm in height and diameter), Young's modulus of 170 Pa and Poisson ratio of 0.2, representing the collagen matrix in the culture model[15, 58]. The external boundaries of the collagen matrix were fixed by prescribing zero displacement. The strains measured experimentally did not exceed 5%, which is well within the limit for linear behavior of collagen[58]. Accordingly, the gel was modeled as a linearly elastic solid.

We modeled isometric tension arising from cellular contractility by prescribing a prestress (p_t) to the epithelial portion. The prestress value was chosen to match the prestrain ($\varepsilon_0 \sim 0.6\%$) found experimentally by measuring the length of initial and detergent-relaxed tubules. Stress tensors were calculated throughout the system, and the maximum principal stress through the midplane of the tubules was visualized and reported.

We modeled changes in cellular contractility within the epithelial tubule by changing the magnitude of the imposed prestress. In particular, to model increased or decreased contractility, we increased or decreased p_t to yield ε_0 of 0.2% or 1%, respectively. These values were determined experimentally by measuring the length of tubules treated with Y27632 or calyculin A before and after relaxation. Similarly, to model a stiffer ECM, we increased the modulus of the matrix portion to match the stiffness of the crosslinked gels at 860 Pa, while keeping the modulus of the epithelial shell fixed at 500 Pa.

Real-time microscopy

For real-time imaging, tubules were constructed of mammary epithelial cells that stably expressed NLS-YFP[46]. Time-lapse movies were collected using a Hamamatsu ECCD camera attached to a Nikon Ti-U inverted microscope customized with a spinning disk (BD Biosciences) and fitted with a humidified environmental chamber held at 37°C and 5% CO_2. Confocal stacks of 20–25 images (2 μm thick) were acquired using a Plan Apo 20× 0.4 NA objective every 15 min beginning at 24 hours after initial microfabrication for a total of 20 hours. Movies were assembled and cells tracked in 3D using ImarisTrack (Bitplane).

Western blot analysis

Samples were lysed using RIPA buffer, mixed with Laemmli sample buffer, heated at 75°C for 5 min, resolved by SDS/PAGE, and transferred to nitrocellulose. Membranes were blocked in 5% milk and incubated overnight at 4°C in 5% milk containing antibodies specific to FAK pY397, total FAK (Invitrogen) or actin (Cell Signaling). Antibodies were visualized using the ECL Plus Western Blotting Detection System (GE Healthcare).

Supplementary Material

Refer to Web version on PubMed Central for supplementary material.

Abbreviations

ECM	extracellular matrix
FAK	focal adhesion kinase
FEM	finite element method
LPA	lyosphosphatidic acid
MLCK	myosin light chain kinase
MMP	matrix metalloproteinase
TGFβ	transforming growth factor-beta
2D	two-dimensional
3D	three-dimensional

Acknowledgments

We thank R. Prud'homme for use of his rheometer, L. Loo for use of her cleanroom, K. Lee and E. Gomez for technical assistance, and J. Tien for helpful discussions. This work was supported by grants from the NIH (GM083997 and CA128660), the David & Lucile Packard Foundation, and Susan G. Komen for the Cure. C.M.N. holds a Career Award at the Scientific Interface from the Burroughs Welcome Fund.

References

1. Affolter M, Bellusci S, Itoh N, Shilo B, Thiery JP, Werb Z. Tube or not tube: remodeling epithelial tissues by branching morphogenesis. Dev. Cell. 2003; 4:11–18. [PubMed: 12530959]
2. Davies, JA. Branching morphogenesis. New York: Landes Bioscience; 2006.
3. Affolter M, Zeller R, Caussinus E. Tissue remodelling through branching morphogenesis. Nat. Rev. Mol. Cell Biol. 2009; 10:831–842. [PubMed: 19888266]
4. Griffith LG, Swartz MA. Capturing complex 3D tissue physiology in vitro. Nat. Rev. Mol. Cell Biol. 2006; 7:211–224. [PubMed: 16496023]
5. Nelson CM, Vanduijn MM, Inman JL, Fletcher DA, Bissell MJ. Tissue geometry determines sites of mammary branching morphogenesis in organotypic cultures. Science. 2006; 314:298–300. [PubMed: 17038622]
6. Nelson CM, Inman JL, Bissell MJ. Three-dimensional lithographically defined organotypic tissue arrays for quantitative analysis of morphogenesis and neoplastic progression. Nat. Protoc. 2008; 3:674–678. [PubMed: 18388950]
7. Silberstein GB, Daniel CW. Reversible inhibition of mammary gland growth by transforming growth factor-beta. Science. 1987; 237:291–293. [PubMed: 3474783]
8. Chen CS, Mrksich M, Huang S, Whitesides GM, Ingber DE. Geometric control of cell life and death. Science. 1997; 276:1425–1428. [PubMed: 9162012]
9. Engler AJ, Sen S, Sweeney HL, Discher DE. Matrix elasticity directs stem cell lineage specification. Cell. 2006; 126:677–689. [PubMed: 16923388]
10. McBeath R, Pirone DM, Nelson CM, Bhadriraju K, Chen CS. Cell shape, cytoskeletal tension, and RhoA regulate stem cell lineage commitment. Dev. Cell. 2004; 6:483–495. [PubMed: 15068789]
11. Nelson CM, Jean RP, Tan JL, Liu WF, Sniadecki NJ, Spector AA, Chen CS. Emergent patterns of growth controlled by multicellular form and mechanics. Proc. Natl. Acad. Sci. U S A. 2005; 102:11594–11599. [PubMed: 16049098]

12. Rauzi M, Lecuit T. Closing in on mechanisms of tissue morphogenesis. Cell. 2009; 137:1183–1184. [PubMed: 19563750]
13. Moore KA, Huang S, Kong Y, Sunday ME, Ingber DE. Control of embryonic lung branching morphogenesis by the Rho activator, cytotoxic necrotizing factor 1. J. Surg. Res. 2002; 104:95–100. [PubMed: 12020126]
14. Moore KA, Polte T, Huang S, Shi B, Alsberg E, Sunday ME, Ingber DE. Control of basement membrane remodeling and epithelial branching morphogenesis in embryonic lung by Rho and cytoskeletal tension. Dev. Dyn. 2005; 232:268–281. [PubMed: 15614768]
15. Paszek MJ, Zahir N, Johnson KR, Lakins JN, Rozenberg GI, Gefen A, Reinhart-King CA, Margulies SS, Dembo M, Boettiger D, Hammer DA, Weaver VM. Tensional homeostasis and the malignant phenotype. Cancer Cell. 2005; 8:241–254. [PubMed: 16169468]
16. Wozniak MA, Desai R, Solski PA, Der CJ, Keely PJ. ROCK-generated contractility regulates breast epithelial cell differentiation in response to the physical properties of a three-dimensional collagen matrix. J. Cell Biol. 2003; 163:583–595. [PubMed: 14610060]
17. Michael L, Sweeney DE, Davies JA. A role for microfilament-based contraction in branching morphogenesis of the ureteric bud. Kidney Int. 2005; 68:2010–2018. [PubMed: 16221201]
18. Bernfield M, Banerjee SD. The turnover of basal lamina glycosaminoglycan correlates with epithelial morphogenesis. Dev Biol. 1982; 90:291–305. [PubMed: 7075863]
19. Williams JM, Daniel CW. Mammary ductal elongation: differentiation of myoepithelium and basal lamina during branching morphogenesis. Dev. Biol. 1983; 97:274–290. [PubMed: 6852366]
20. Ingber, DE.; Jamieson, JD. Gene expression during normal and malignant differentiation. Andersson, LC.; Gahmberg, CG.; Ekblom, P., editors. Orlando, FL: Academic Press; 1985. p. 13-32.
21. Beloussov LV, Dorfman JG, Cherdantzev VG. Mechanical stresses and morphological patterns in amphibian embryos. J Embryol Exp Morphol. 1975; 34:559–574. [PubMed: 1082486]
22. Alcaraz J, Xu R, Mori H, Nelson CM, Mroue R, Spencer VA, Brownfield D, Radisky DC, Bustamante C, Bissell MJ. Laminin and biomimetic extracellular elasticity enhance functional differentiation in mammary epithelia. Embo J. 2008; 27:2829–2838. [PubMed: 18843297]
23. Lee J, Leonard M, Oliver T, Ishihara A, Jacobson K. Traction forces generated by locomoting keratocytes. J. Cell Biol. 1994; 127:1957–1964. [PubMed: 7806573]
24. Pelham RJ Jr, Wang Y. High resolution detection of mechanical forces exerted by locomoting fibroblasts on the substrate. Mol. Biol. Cell. 1999; 10:935–945. [PubMed: 10198048]
25. Davies SP, Reddy H, Caivano M, Cohen P. Specificity and mechanism of action of some commonly used protein kinase inhibitors. Biochem. J. 2000; 351:95–105. [PubMed: 10998351]
26. Ishihara H, Martin BL, Brautigan DL, Karaki H, Ozaki H, Kato Y, Fusetani N, Watabe S, Hashimoto K, Uemura D, et al. Calyculin A and okadaic acid: inhibitors of protein phosphatase activity. Biochem. Biophys. Res. Commun. 1989; 159:871–877. [PubMed: 2539153]
27. Provenzano PP, Inman DR, Eliceiri KW, Keely PJ. Matrix density-induced mechanoregulation of breast cell phenotype, signaling and gene expression through a FAK-ERK linkage. Oncogene. 2009
28. Levental KR, Yu H, Kass L, Lakins JN, Egeblad M, Erler JT, Fong SF, Csiszar K, Giaccia A, Weninger W, Yamauchi M, Gasser DL, Weaver VM. Matrix crosslinking forces tumor progression by enhancing integrin signaling. Cell. 2009; 139:891–906. [PubMed: 19931152]
29. Fischer RS, Gardel M, Ma X, Adelstein RS, Waterman CM. Local cortical tension by myosin II guides 3D endothelial cell branching. Curr Biol. 2009; 19:260–265. [PubMed: 19185493]
30. Mammoto A, Connor KM, Mammoto T, Yung CW, Huh D, Aderman CM, Mostoslavsky G, Smith LE, Ingber DE. A mechanosensitive transcriptional mechanism that controls angiogenesis. Nature. 2009; 457:1103–1108. [PubMed: 19242469]
31. Girton TS, Oegema TR, Tranquillo RT. Exploiting glycation to stiffen and strengthen tissue equivalents for tissue engineering. J. Biomed. Mater. Res. 1999; 46:87–92. [PubMed: 10357139]
32. Adams CL, Nelson WJ. Cytomechanics of cadherin-mediated cell-cell adhesion. Curr. Opin. Cell Biol. 1998; 10:572–577. [PubMed: 9818166]
33. Gottardi CJ, Gumbiner BM. Adhesion signaling: how beta-catenin interacts with its partners. Curr. Biol. 2001; 11:R792–R794. [PubMed: 11591340]

34. Schlaepfer DD, Mitra SK. Multiple connections link FAK to cell motility and invasion. Curr. Opin. Genet. Dev. 2004; 14:92–101. [PubMed: 15108811]
35. Nagy T, Wei H, Shen TL, Peng X, Liang CC, Gan B, Guan JL. Mammary epithelial-specific deletion of the focal adhesion kinase gene leads to severe lobulo-alveolar hypoplasia and secretory immaturity of the murine mammary gland. J. Biol. Chem. 2007; 282:31766–31776. [PubMed: 17716968]
36. van Miltenburg MH, Lalai R, de Bont H, van Waaij E, Beggs H, Danen EH, van de Water B. Complete focal adhesion kinase deficiency in the mammary gland causes ductal dilation and aberrant branching morphogenesis through defects in Rho kinase-dependent cell contractility. Faseb J. 2009; 23:3482–3493. [PubMed: 19584305]
37. Tang D, Mehta D, Gunst SJ. Mechanosensitive tyrosine phosphorylation of paxillin and focal adhesion kinase in tracheal smooth muscle. Am. J. Physiol. 1999; 276:C250–C258. [PubMed: 9886941]
38. Yano Y, Geibel J, Sumpio BE. Tyrosine phosphorylation of pp125FAK and paxillin in aortic endothelial cells induced by mechanical strain. Am. J. Physiol. 1996; 271:C635–C649. [PubMed: 8770005]
39. Chang F, Lemmon CA, Park D, Romer LH. FAK potentiates Rac1 activation and localization to matrix adhesion sites: a role for betaPIX. Mol. Biol. Cell. 2007; 18:253–264. [PubMed: 17093062]
40. Gomez EW, Chen QK, Gjorevski N, Nelson CM. Tissue geometry patterns epithelial-mesenchymal transition via intercellular mechanotransduction. J. Cell. Biochem. 2010; 110:44–51. [PubMed: 20336666]
41. Lu P, Werb Z. Patterning mechanisms of branched organs. Science. 2008; 322:1506–1509. [PubMed: 19056977]
42. Alsberg, E.; Moore, K.; Huang, S.; Polte, T.; Ingber, DE. Lung development and regeneration. Massaro, DJ.; Massaro, GD.; Chambon, P., editors. New York: Marcel Dekker; 2004. p. 247-274.
43. Kanwar YS, Ota K, Yang Q, Wada J, Kashihara N, Tian Y, Wallner EI. Role of membrane-type matrix metalloproteinase 1 (MT-1-MMP), MMP-2, and its inhibitor in nephrogenesis. Am. J. Physiol. 1999; 277:F934–F947. [PubMed: 10600941]
44. Meyer TN, Schwesinger C, Bush KT, Stuart RO, Rose DW, Shah MM, Vaughn DA, Steer DL, Nigam SK. Spatiotemporal regulation of morphogenetic molecules during in vitro branching of the isolated ureteric bud: toward a model of branching through budding in the developing kidney. Dev. Biol. 2004; 275:44–67. [PubMed: 15464572]
45. Wiseman BS, Sternlicht MD, Lund LR, Alexander CM, Mott J, Bissell MJ, Soloway P, Itohara S, Werb Z. Site-specific inductive and inhibitory activities of MMP-2 and MMP-3 orchestrate mammary gland branching morphogenesis. J. Cell Biol. 2003; 162:1123–1133. [PubMed: 12975354]
46. Mori H, Gjorevski N, Inman JL, Bissell MJ, Nelson CM. Self-organization of engineered epithelial tubules by differential cellular motility. Proc. Natl. Acad. Sci. U S A. 2009; 106:14890–14895. [PubMed: 19706461]
47. Prajapati RT, Chavally-Mis B, Herbage D, Eastwood M, Brown RA. Mechanical loading regulates protease production by fibroblasts in three-dimensional collagen substrates. Wound Repair Regen. 2000; 8:226–237. [PubMed: 10886813]
48. Ruddy JM, Jones JA, Stroud RE, Mukherjee R, Spinale FG, Ikonomidis JS. Differential effects of mechanical and biological stimuli on matrix metalloproteinase promoter activation in the thoracic aorta. Circulation. 2009; 120:S262–S268. [PubMed: 19752377]
49. Hanks SK, Ryzhova L, Shin NY, Brabek J. Focal adhesion kinase signaling activities and their implications in the control of cell survival and motility. Front. Biosci. 2003; 8:d982–d996. [PubMed: 12700132]
50. Gill SE, Pape MC, Leco KJ. Tissue inhibitor of metalloproteinases 3 regulates extracellular matrix--cell signaling during bronchiole branching morphogenesis. Dev. Biol. 2006; 298:540–554. [PubMed: 16890932]
51. Kouros-Mehr H, Werb Z. Candidate regulators of mammary branching morphogenesis identified by genome-wide transcript analysis. Dev. Dyn. 2006; 235:3404–3412. [PubMed: 17039550]

52. Janda E, Lehmann K, Killisch I, Jechlinger M, Herzig M, Downward J, Beug H, Grunert S. Ras and TGF[beta] cooperatively regulate epithelial cell plasticity and metastasis: dissection of Ras signaling pathways. J. Cell Biol. 2002; 156:299–313. [PubMed: 11790801]

53. Janda E, Nevolo M, Lehmann K, Downward J, Beug H, Grieco M. Raf plus TGFbeta-dependent EMT is initiated by endocytosis and lysosomal degradation of E-cadherin. Oncogene. 2006; 25:7117–7130. [PubMed: 16751808]

54. Brown KA, Aakre ME, Gorska AE, Price JO, Eltom SE, Pietenpol JA, Moses HL. Induction by transforming growth factor-beta1 of epithelial to mesenchymal transition is a rare event in vitro. Breast Cancer Res. 2004; 6:R215–R231. [PubMed: 15084245]

55. Oft M, Peli J, Rudaz C, Schwarz H, Beug H, Reichmann E. TGF-beta1 and Ha-Ras collaborate in modulating the phenotypic plasticity and invasiveness of epithelial tumor cells. Genes Dev. 1996; 10:2462–2477. [PubMed: 8843198]

56. Boyd NF, Guo H, Martin LJ, Sun L, Stone J, Fishell E, Jong RA, Hislop G, Chiarelli A, Minkin S, Yaffe MJ. Mammographic density and the risk and detection of breast cancer. N. Engl. J. Med. 2007; 356:227–236. [PubMed: 17229950]

57. Paszek MJ, Weaver VM. The tension mounts: mechanics meets morphogenesis and malignancy. J. Mammary Gland Biol. Neoplasia. 2004; 9:325–342. [PubMed: 15838603]

58. Barocas VH, Moon AG, Tranquillo RT. The fibroblast-populated collagen microsphere assay of cell traction force--Part 2: Measurement of the cell traction parameter. J. Biomech. Eng. 1995; 117:161–170. [PubMed: 7666653]

59. Khaled WT, Read EK, Nicholson SE, Baxter FO, Brennan AJ, Came PJ, Sprigg N, McKenzie AN, Watson CJ. The IL-4/IL-13/Stat6 signalling pathway promotes luminal mammary epithelial cell development. Development. 2007; 134:2739–2750. [PubMed: 17611223]

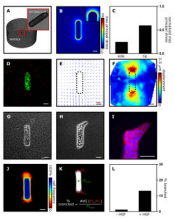

Fig. 1. Patterns of mechanical stress correspond to sites of branching in epithelial tissues

(A) FEM mesh, showing the cellular (epithelium) and ECM (matrix) portions of the stress model. **(B, C)** FEM stress profile of an epithelial tubule. **(D)** Fluorescent image of engineered mammary epithelial tubule showing cellular membranes (green) and microbeads (red) embedded in the surrounding collagen gel. **(E)** Map of bead displacements around a single engineered tubule and **(F)** average displacements around 15 tubules. **(G)** Phase contrast image of engineered tubule before induction of branching. **(H)** Phase contrast image, **(I)** fluorescent image of E-cadherin (red) and nuclei (blue), and **(J)** frequency map of engineered tubules after induction of branching. **(K, L)** Branching is quantified by measuring the pixel intensity (PI) at a fixed location away from the tip in the grayscale frequency map, and then calculating the percent of tubules that have extended branches. Scale bars, 50 μm; displacement scale bar (red), 3 μm.

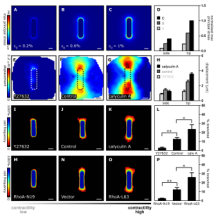

Fig. 2. Patterns of mechanical stress and branching morphogenesis are affected by cellular contractility

Mechanical stress profiles of tubules with increasing contractility: prestress (p_t) that yields prestrain (ε_0) of **(A)** 0.2 % **(B)** 0.6 % **(C)** 1% and **(D)** combined stress profiles. **(E–H)** Matrix displacement maps around control tubules and tubules treated with 10 μM Y27632 or 0.1 nM calyculin A. **(I–K)** Frequency maps of branching from control tubules and tubules treated with 10 μM Y27632 or 0.1 nM calyculin A. **(L)** Branching was also quantified by measuring the pixel intensity 12 μm away from the tubule tip. Branch frequency decreases when tubules are treated with Y27632, and increases when tubules are treated with calyculin A. **(M–O)** Frequency maps and **(P)** quantification of branching from tubules constructed of cells transduced with adenovirus encoding RhoA-N19, RhoA-L63, or control vector. *p<0.05; **p<0.01; Scale bars, 50 μm.

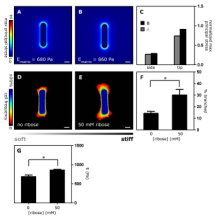

Fig. 3. Patterns of mechanical stress and branching morphogenesis are affected by matrix stiffness

Mechanical stress profiles of tubules surrounded by matrices of different stiffness: **(A)** E_{matrix} = 680 Pa, **(B)** E_{matrix} = 860 Pa and **(C)** combined stress profiles. Frequency maps of branching tubules embedded in collagen gel crosslinked with **(D)** 0 and **(E)** 50 mM D-ribose. **(F)** Branch frequency increases as the stiffness of the collagen gel increases **(G)**. Rheological measurements of collagen gels crosslinked with D-ribose. *p<0.05; Scale bars, 50 μm.

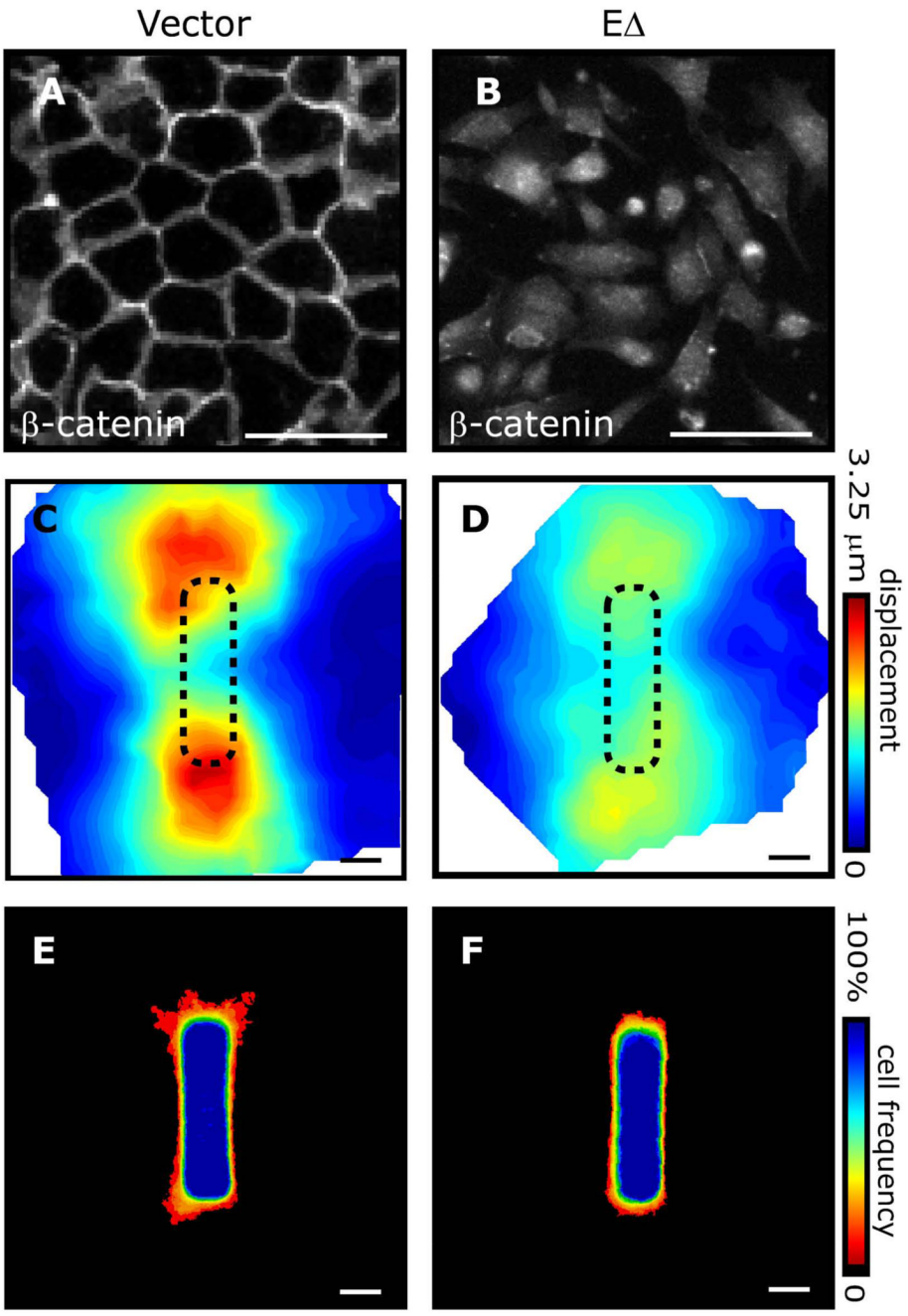

Fig. 4. Intercellular cohesion is required for patterning stress and branching morphogenesis

β-catenin immunofluorescence in **(A)** control mammary epithelial cells and **(B)** cells expressing EΔ. Matrix displacement maps following relaxation of **(C)** control tubules and **(D)** tubules expressing EΔ. Frequency maps of branching from **(E)** control tubules and **(F)** tubules expressing EΔ. Scale bars, 50 μm.

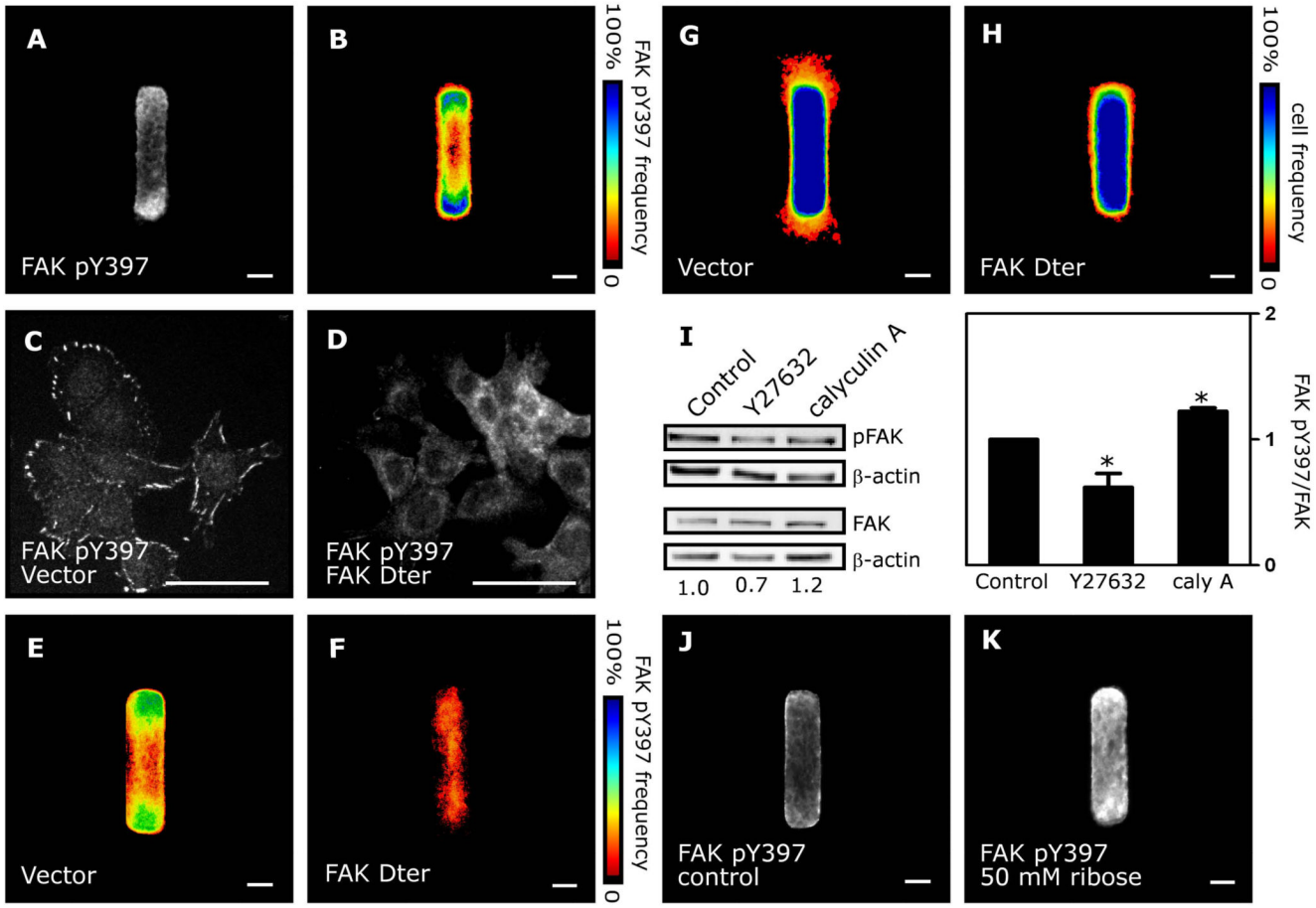

Fig. 5. FAK is activated at tips of tubules and required for branching morphogenesis

(A) FAK pY397 immunofluorescence and **(B)** frequency map in engineered tubules. FAK pY397 immunofluorescence in **(C)** control cells and **(D)** cells expressing FAK Dter. Frequency maps of FAK pY397 in **(E)** control tubules and **(F)** tubules expressing FAK Dter. Frequency map of branching from **(G)** control tubules and **(H)** tubules expressing FAK Dter. **(I)** Western blot analysis of FAK pY397 and total FAK in tubules treated with Y27632 or calyculin A. FAK pY397 immunofluorescence in **(J)** control tubules and **(K)** tubules constructed in collagen crosslinked using ribose. *p<0.05; Scale bars, 50 μm.

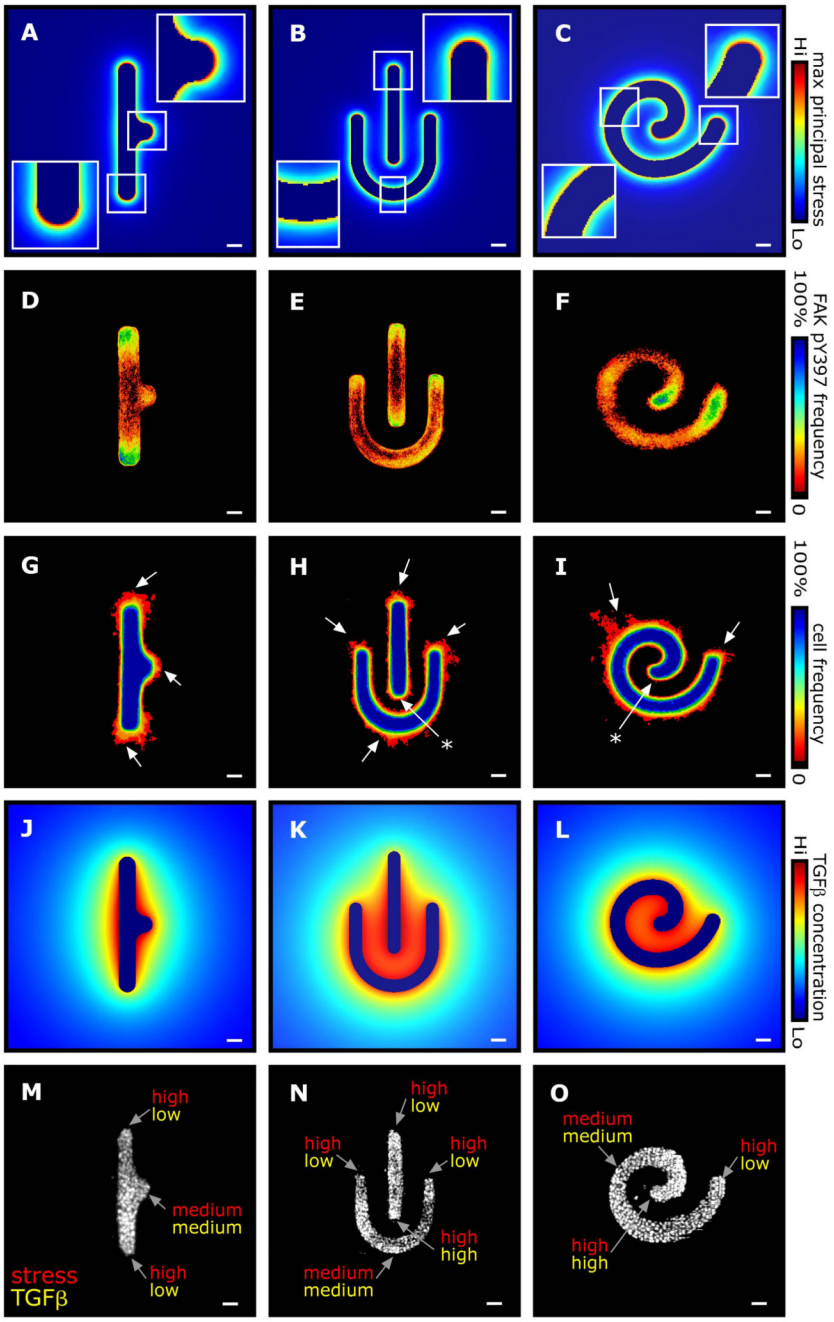

Fig. 6. Patterns of mechanical stress and branching morphogenesis are affected by tissue geometry

(A–C) FEM stress profiles of tubules of various geometry. Frequency maps of **(D–F)** FAK pY397 immunofluorescence and **(G–I)** branching from tubules of the corresponding geometries. Arrows denote regions of high mechanical stress that branch, and asterisks denote regions of high mechanical stress that do not branch. **(J–L)** Predicted concentration profiles of TGFβ around tubules of various geometry. **(M–O)** Relative strength of the mechanical and biochemical inputs as a function of position within the tissue. Scale bars, 50 μm.